Article ID: 1671-3664(2002)02-0167-14

Influence of earthquake ground motion incoherency on multi-support structures

Yang Qingshan (杨庆山)[1†] , M. Saiid Saiidi[2†] , Wang Hang (王　航) [3‡] and Ahmad Itani[4§]

1. *School of Civil Engineering and Architecture, Northern Jiaotong University, Beijing, 100044, China,*

2. *Department of Civil Engineering, University of Nevada, Reno, NV, 89557,USA*

3. *Beijing General Municipal Engineering Design and Research Institute, China*

4.*Department of Civil Engineering, University of Nevada, Reno, NV, 89557, USA*

Abstract: A linear response history analysis method is used to determine the influence of three factors: geometric incoherency, wave-passage, and local site characteristics on the response of multi-support structures subjected to differential ground motions. A one-span frame and a reduced model of a 24-span bridge, located in Las Vegas, Nevada are studied, in which the influence of each of the three factors and their combinations are analyzed. It is revealed that the incoherency of earthquake ground motion can have a dramatic influence on structural response by modifying the dynamics response to uniform excitation and inducing pseudo-static response, which does not exist in structures subjected to uniform excitation. The total response when all three sources of ground motion incoherency are included is generally larger than that of uniform excitation.

Keywords: earthquake; bridges; ground motion; incoherency; wave passage; local site characteristics; multi-support structures

1 Introduction

In earthquake response analysis, traditionally it has been assumed that all points of the ground surface beneath the foundation are excited synchronously and experience the same ground motion. It has been well known from real earthquake records that the earthquake ground motions vary both temporally and spatially, and it has been believed that the spatial variability of seismic ground motions can have an important effect on the response of bridges and other multi-support structures. This is because, in addition to the dynamic response, a pseudo-static response is introduced by the spatially varying ground motions. The pseudo-static effects that arise from spatial variation of ground motion cannot be addressed in coherent ground motion analysis of the structure.

To find rational and substantiated answers to the influence of incoherent ground motions, two aspects need to be covered in sequence, 1) a sufficient knowledge of the mechanisms underlying the spatial variability of the motion, 2) assessment through numerical and experimental studies of the relevance of this knowledge on the response, in terms sufficiently articulated to be used for design.

A breakthrough in collecting data on coherency function occurred (Abrahamsom, 1987) with the installation of strong-motion arrays, such as SMART-1, Lotung LSST, and SMART-2 (Abrahamson, 1987; Beresnev *et al*., 1994), to address the first aspect. Studies on the response of bridges and other multi-support structures subjected to different motions were started more than 30 years ago (Bodganoff *et al*., 1965; Luco and Wong, 1986; Perotti, 1990; Zerva, 1990; Hao, 1998, 1999; Harichandran *et al*., 1996; Kahan *et al*., 1996; Shrikhande and Gupta, 1999; Ettouney *et al*., 2001; Nazmy and Abdel-Ghaffar, 1992; Abdel-Ghaffar and Nazmy, 1991; Price, 1998; Behnamfar, 1999). Most of the studies have shown multiple-support seismic excitation can have a significant effect on the structural response. However, there are still important issues related to modeling of incoherency, the influence of local site effects, and the effect of combination of different incoherency sources that require further studies. This paper focuses on the influence of three factors, geometric incoherency, wave-passage, and local site condition, on the response of multi-support linear structures using response history analysis. The coherency model of ground motions and the method of generating coherent ground motions based on phase difference

Correspondence to: M. Saiid Saiidi, Department of Civil Engineering, University of Nevad, Reno, NV, 89577
Tel: 775-784-4839; Fax: 775-784-1390;
Email: saiidi@unr.edu
[†]Professor; [‡]Engineer; [§]Associate Professor

spectra are summarized (Yang and Chen, 2000; Yang and Jiang, 2001). A one-span frame and a reduced model of a 24-span bridge, located in Las Vegas, Nevada are studied and the influence of each of the three factors and their combinations are analyzed.

2 Analytical modeling

2.1 Equilibrium equations

For the sake of simplicity, it is assumed that structures behave in a linear elastic fashion. For a finite element model of multi-support structures, the equation of motion is:

$$\begin{bmatrix} \boldsymbol{m}_{aa} & \boldsymbol{m}_{ab} \\ \boldsymbol{m}_{ba} & \boldsymbol{m}_{bb} \end{bmatrix} \begin{Bmatrix} \ddot{\boldsymbol{x}}_a \\ \ddot{\boldsymbol{x}}_b \end{Bmatrix} + \begin{bmatrix} \boldsymbol{c}_{aa} & \boldsymbol{c}_{ab} \\ \boldsymbol{c}_{ba} & \boldsymbol{c}_{bb} \end{bmatrix} \begin{Bmatrix} \dot{\boldsymbol{x}}_a \\ \dot{\boldsymbol{x}}_b \end{Bmatrix} + \begin{bmatrix} \boldsymbol{k}_{aa} & \boldsymbol{k}_{ab} \\ \boldsymbol{k}_{ba} & \boldsymbol{k}_{bb} \end{bmatrix} \begin{Bmatrix} \boldsymbol{x}_a \\ \boldsymbol{x}_b \end{Bmatrix} = \begin{Bmatrix} \boldsymbol{P}_a \\ \boldsymbol{P}_b \end{Bmatrix} \tag{1}$$

in which $\boldsymbol{m}$, $\boldsymbol{c}$, $\boldsymbol{k}$ are mass, damping, and stiffness matrices, respectively; $\boldsymbol{P}$ is the external force or the reaction vector, and $\ddot{\boldsymbol{x}}$, $\dot{\boldsymbol{x}}$ and $\boldsymbol{x}$ are the absolute acceleration, velocity, and displacement responses relative to the inertia coordinate system, respectively. The subscripts a and b refer to the structure and the supports, respectively. The equation for response may be written as:

$$\begin{aligned} &\boldsymbol{m}_{aa}\ddot{\boldsymbol{x}}_a + \boldsymbol{c}_{aa}\dot{\boldsymbol{x}}_a + \boldsymbol{k}_{aa}\boldsymbol{x}_a \\ &= \boldsymbol{P}_a - \left(\boldsymbol{m}_{ab}\ddot{\boldsymbol{x}}_b + \boldsymbol{c}_{ab}\dot{\boldsymbol{x}}_b + \boldsymbol{k}_{ab}\boldsymbol{x}_b\right) \end{aligned} \tag{2}$$

The response $\boldsymbol{x}_a$ in linear structure may be described as the sum of two components:

$$\boldsymbol{x}_a = \boldsymbol{x}_{da} + \boldsymbol{x}_{sa} \tag{3}$$

where $\boldsymbol{x}_{da}$ is the dynamic responses and $\boldsymbol{x}_{sa}$ is the pseudo-static response, which results from the differential support displacements. Substituting Eq.(3) into Eq.(2) will lead to:

$$\begin{aligned} &\boldsymbol{m}_{aa}\ddot{\boldsymbol{x}}_{da} + \boldsymbol{c}_{aa}\dot{\boldsymbol{x}}_{da} + \boldsymbol{k}_{aa}\boldsymbol{x}_{da} \\ &= \boldsymbol{P}_a - \left[\left(\boldsymbol{m}_{aa}\ddot{\boldsymbol{x}}_{sa} + \boldsymbol{m}_{ab}\ddot{\boldsymbol{x}}_b\right) + \left(\boldsymbol{c}_{aa}\dot{\boldsymbol{x}}_{sa} + \boldsymbol{c}_{ab}\dot{\boldsymbol{x}}_b\right)\right. \\ &\quad \left. + \left(\boldsymbol{k}_{aa}\boldsymbol{x}_{sa} + \boldsymbol{k}_{ab}\boldsymbol{x}_b\right)\right] \end{aligned} \tag{4}$$

in which there are two unknown vectorsand $\boldsymbol{x}_{da}$ and $\boldsymbol{x}_{sa}$. To solve Eq.(4), the static equilibrium equation for the pseudo-static response is needed. From structural analysis, there is:

$$\boldsymbol{x}_{sa} = -\boldsymbol{k}_{aa}^{-1}\boldsymbol{k}_{ab}\boldsymbol{x}_b = -\boldsymbol{R}\boldsymbol{x}_b \tag{5}$$

Where $\boldsymbol{R} = -\boldsymbol{K}_{aa}^{-1}\boldsymbol{K}_{ab}$. Substitute Eq.(5) into Eq.(4) then

$$\begin{aligned} &\boldsymbol{m}_{aa}\ddot{\boldsymbol{x}}_{da} + \boldsymbol{c}_{aa}\dot{\boldsymbol{x}}_{da} + \boldsymbol{k}_{aa}\boldsymbol{x}_{da} \\ &= \boldsymbol{P}_a - \left(-\boldsymbol{m}_{aa}\boldsymbol{R} + \boldsymbol{m}_{ab}\right)\ddot{\boldsymbol{x}}_b - \left(-\boldsymbol{c}_{aa}\boldsymbol{R} + \boldsymbol{c}_{ab}\right)\dot{\boldsymbol{x}}_b \end{aligned} \tag{6}$$

Since the physical damping matrix on the right hand side of the equation is almost impossible to define, that part of the damping force is normally neglected (Wilson, 2000), Therefore,

$$\begin{aligned} &\boldsymbol{m}_{aa}\ddot{\boldsymbol{x}}_{da} + \boldsymbol{c}_{aa}\dot{\boldsymbol{x}}_{da} + \boldsymbol{k}_{aa}\boldsymbol{x}_{da} \\ &= \boldsymbol{P}_a - \left(-\boldsymbol{m}_{aa}\boldsymbol{R} + \boldsymbol{m}_{ab}\right)\ddot{\boldsymbol{x}}_b \end{aligned} \tag{7}$$

For lumped-mass system, $\boldsymbol{m}_{ab} = 0$, then the equation may be simplified as:

$$\begin{aligned} &\boldsymbol{m}_{aa}\ddot{\boldsymbol{x}}_{da} + \boldsymbol{c}_{aa}\dot{\boldsymbol{x}}_{da} + \boldsymbol{k}_{aa}\boldsymbol{x}_{da} \\ &= \boldsymbol{P}_a + \boldsymbol{m}_{aa}\boldsymbol{R}\ddot{\boldsymbol{x}}_b \end{aligned} \tag{8}$$

Eq.(8) is the fundamental equation for the response of structure subjected to non-uniform earthquake ground motions.

2.2 Generation of coherent ground motions

To obtain the structural responses from Eqs. (5) and (8), a suite of coherent ground motion should be generated first. The stochastic field may be generated according to the spectral representation method and the jth stationary response history of the space-time random field with zero mean value may be simulated through (Hao, 1989):

$$U^j(t) = \sum_{m=1}^{n}\sum_{k=0}^{N-1} a_m^j(\omega_k)\cos\left[\omega_k t + \theta_m^j(\omega_k) + \varphi_{mk}\right] \tag{9}$$

where amplitude $a_m^j(\omega_k)$ and phase angle $\theta_m^j(\omega_k)$ are determined by complex LL^T decomposition of the cross-power spectral density matrix of the ground accelerations; φ_m is a set of independent random phase angles uniformly distributed in $(0, 2\pi)$.

To consider the non-stationarity of earthquake ground motions, random phase angle φ_m will be modified in this work to be uniformly but not independently distributed in $(0, 2\pi)$. The correlation for φ_m is specified by phase difference spectra (Yang and Jiang, 2001). The cross-power spectral density matrix is specified by:

$$G_{kl}(f) = \rho_{kl}(f, d)\sqrt{G_k(f)G_l(f)} \tag{10}$$

where f denotes the frequency; $G_k(f)$ and $G_l(f)$ denote the auto-power spectral densities of the processes at locations k and l, respectively; $\rho_{kl}(d, f)$ is the coherency function of ground accelerations between two locations k and l at a distance d; and $G_{kl}(f)$ denotes the cross-power spectral density of the processes at these two locations.

2.2.1 Incoherency model of ground motions

From a physical point of view, the spatial variation of seismic ground motion may be schematically thought to be the result of the combination of three different phenomena: (1) the incoherency effect resulting from reflections and refractions of waves through the soil during their propagation (this effect is referred to as "geometric incoherency"); (2) the wave-passage effect, which is the difference in the arrival times of seismic waves at different locations; and (3) the local site effect due to differences in local soil conditions under various supports.

A theoretical model for the coherency function describing the spatial variability of earthquake ground motions was developed in Der Kiureghian (1996), based on basic principles of random processes and some simplifying assumptions regarding the propagation of seismic waves:

$$\rho(f,d)=\rho(f,d)^{\text{geom}}\cdot\rho(f,d)^{\text{wave}}\cdot\rho(f,d)^{\text{site}} \tag{11}$$

where $\rho(f,d)^{\text{geom}}$, $\rho(f,d)^{\text{wave}}$ and $\rho(f,d)^{\text{site}}$ denote the 'geometric incoherency' effect, the 'wave-passage' effect, and the 'local-site' effect, respectively.

Because this model is broadly accepted (Price, 1998; Shrikhande and Gupta, 1999; Banerji *et al*., 2000), the geometric incoherency effect of this model, i.e., the lagged coherency, specified based on SMART-1 recordings (Yang and Chen, 2000), was adopted in the present work:

$$\begin{aligned}\rho(d,f)^{\text{geom}} &= \cos(\arctan(a_1 d^{0.25}+a_2(df)^{0.5}))\cdot \\ &\quad \exp((-0.5(a_3 d^{a_4} f^{a_5})^2) \\ &= (1+(a_1 d^{0.25}+a_2(df)^{0.5}))^{-0.5}\cdot \\ &\quad \exp((-0.5(a_3 d^{a_4} f^{a_5})^2)\end{aligned} \tag{12}$$

where a_1=0.115144, a_2=-0.224874×10^{-2}, a_3= 0.762306×10^{-1}, a_4=0.378401 a_5=0.220597 are the regressive parameters (Yang and Chen, 2000). Note that even though SMART-1 incoherency effects were obtained at the ground surface, they were used in the present study for the bedrock because the topsoil at the site of SMART-1 was nearly uniform. Wave passage and local-site effect were considered separately by means of response history analysis.

2.2.2 Power spectral density

The power spectral density (PSD) function adopted in this work is the modified Kanai-Tajimi spectrum of ground accelerations (Clough and Penzien, 1975) and is expressed as:

$$S(\omega)=S_{\text{CP}}(\omega)S_0=\frac{\omega_{\text{g}}^4+4\xi_{\text{g}}^2\omega_{\text{g}}^2\omega^2}{\left(\omega^2-\omega_{\text{g}}^2\right)^2+4\xi_{\text{g}}^2\omega_{\text{g}}^2\omega^2}\times \frac{\omega^4}{(\omega^2-\omega_{\text{f}}^2)^2+4\xi_{\text{f}}^2\omega_{\text{f}}^2\omega^2}S_0 \tag{13}$$

where ω is the circular frequency; S_0 is scale factor; $S_{\text{CP}}(\omega)$ is the normalized Clough-Penzien spectrum; ω_{g} and ξ_{g} are the characteristic ground frequency and damping; ω_{f} and ξ_{f} are the parameters of an additional filter, introduced to assure finite power for the PSD. Parameters may be determined following the procedures in (Monti *et al*., 1996).

2.2.3 Random phase angle and phase difference spectrum

In most procedures for generating earthquake ground motions, the random phase angle of the trigonometric approximation has been assumed to be an independent random variable with uniform distribution in $(0, 2\pi)$ (Ohsaki, 1979) and a stationary process is obtained. To account for the non-stationary nature of ground accelerations, the stationary time histories were modulated by means of an envelope function (Monti *et al*., 1996), while the frequency nonstationarity, due to the different arrival time of push, shear, and surface waves that propagate at different velocities through the earth crust, has rarely been taken into account in generating artificial ground motions.

Both the time and frequency nonstationarities of the real earthquake ground motions are taken into account in the present work by means of determining random phase angle φ_k through phase difference spectrum $\Delta\varphi_k$ (Ohsaki, 1979):

$$\varphi_{k+1}(f)=\varphi_k(f)+\Delta\varphi_k(f)$$

$$\varphi_k\in[0,2\pi] \qquad k=0,\quad 1,\cdots n-1 \tag{14}$$

$$\Delta\varphi_k(f)=\Delta\overline{\varphi}_k(f)+\varepsilon_k \qquad \Delta\varphi_k(f)\in[-2\pi,0]$$

$$k=0,\quad 1,\cdots n-1 \tag{15}$$

and any value in domain $(0, 2\pi]$ may be specified as the initial phase angle φ_0. $\Delta\overline{\varphi}_k(f)$ is the mean function of phase difference spectrum and ε_k the fluctuating part of the phase difference spectrum around the mean function. The empirical relation of $\Delta\overline{\varphi}_k(f)$ to its influence factors is:

$$\log_{10}\left|\Delta\overline{\varphi}(f)\right|=a_1(f)+a_2(f)\cdot M+a_3(f)\log_{10}(R+R_0) \tag{16}$$

and

$$\Delta\bar{\varphi}(f) = -\left|\Delta\bar{\varphi}(f)\right| < 0 \tag{17}$$

where M is the earthquake magnitude; R is the epicenter distance in km; R_0 =15 is a constant. $a_1(f)$, $a_2(f)$, $a_3(f)$ are regressive coefficients as functions of frequency (Zhao, 1992). ε_k is the fluctuating part of the phase difference spectrum around the mean function and can be obtained from (Yang and Jiang, 2001):

$$\varepsilon_k = -(\varepsilon_{bk} - 2\pi) \tag{18}$$

where $\varepsilon_{bk} = e^{\varepsilon_{ck}}$ and ε_{ck} is a random variable satisfying the normal distribution law with mean value m_c and standard deviation σ_c which can be calculated from:

$$m_c = \ln 2\pi - \frac{1}{2}\ln(1 + (\frac{\sigma_\varepsilon}{2\pi})^2) \tag{19.a}$$

$$\sigma_c = \ln(1 + (\frac{\sigma_\varepsilon}{2\pi})^2) \tag{19.b}$$

in which σ_ε is the standard deviation of random variable ε_k and:

$$\log_{10}\sigma_\varepsilon = d_1 + d_2 \cdot M + d_3 \log_{10}(R + R_0) \tag{20}$$

where d_1, d_2, d_3 are coefficients and $d_1 = -1.124$, $d_2 = 0.089$, $d_3 = 0.316$ for bedrock site (Zhao, 1992); the other symbols are the same as those in Eq. 16.

After the amplitude a_m, phase angle θ_m and random phase angle φ_m are specified, Fast Fourier Transform is applied to Eq. 9 and the artificial nonstationary ground motions are obtained (Yang and Jiang, 2001).

3 Effect of incoherent ground motion in one-span frame

To develop a general understanding of the influence of incoherency of ground motions on the longitudinal response of multi-support structures, a one-span two-support frame is first studied. The system under consideration is presented in Fig.1. It is assumed that the earthquake waves arrive at supports *A* and *D* from the source in three steps: 1) earthquake waves arrive at point 1 and 2 synchronically, but the waves are different due to geometric incoherency; 2) earthquake wave travels from point 1 to point 1', where wave-passage effect is induced; 3) earthquake waves pass through top soil and reach points *A* and *D* from 1' and 2, respectively, where local site effect is resulted. Note that 1 and 2 have the same focal distances. The above three steps introduce three types of incoherency, all of which have to be included in a comprehensive evaluation of the effects of incoherent ground motions. The influence of each of them and their combination will be analyzed one by one.

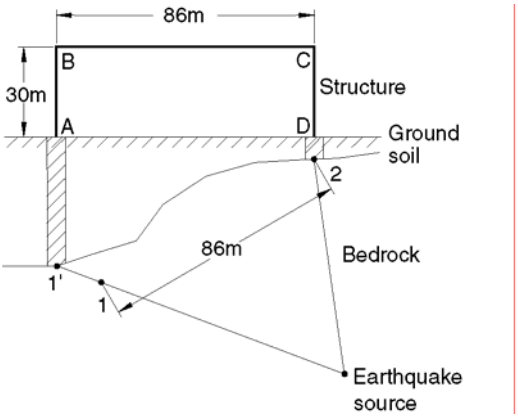

Fig. 1 One-span two-support frame structure-soil system

3.1 Coherent ground motions

To consider the influence of each incoherency factor, two artificial ground motions at a deep rock site are generated at points 1 and 2. It is assumed that the earthquake magnitude is 7.4 and the epicenter distance is 40 km. The acceleration histories of two points spaced 86 m on bedrock satisfying the coherent function Eq.(12) may be generated following the procedures shown in Section 2.2. The PSD is presented in Fig.2.

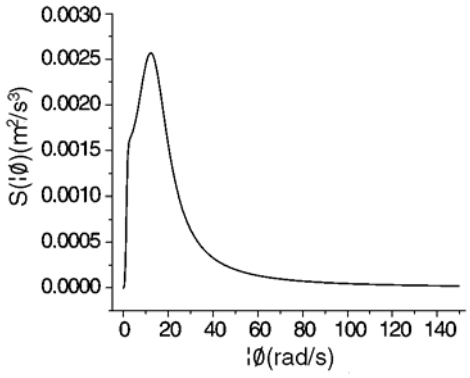

Fig. 2 Power spectrum density

The generated ground accelerations are denoted as Acc.1 and Acc.2. Fig.3 compares the target and simulated incoherency functions. The corresponding displacement records, Disp.1 and Disp.2, are obtained by integration. Acc.1 and Disp.1 are presented in Fig. 4.

3.2 Parametric studies

After matrices ***m***, ***c***, ***k*** and the ground motions are obtained, the structural response is determined by the Wilson-θ method. Sixty cases are analyzed to study the influence of geometric incoherency, wave-passage, and local site on internal moment.

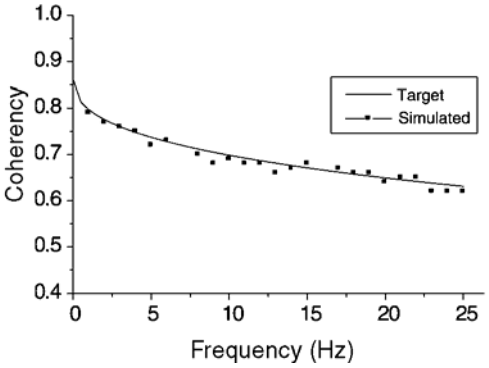

Fig. 3 Comparison of simulated and target incoherency functions

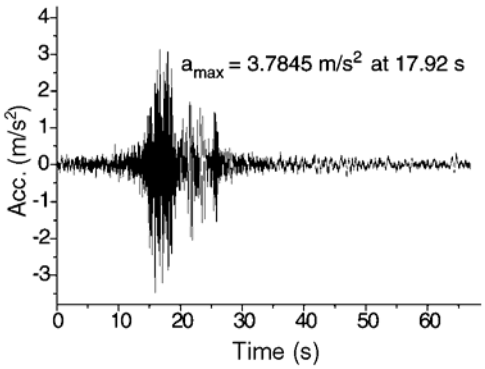

(a) Acceleration Acc.1

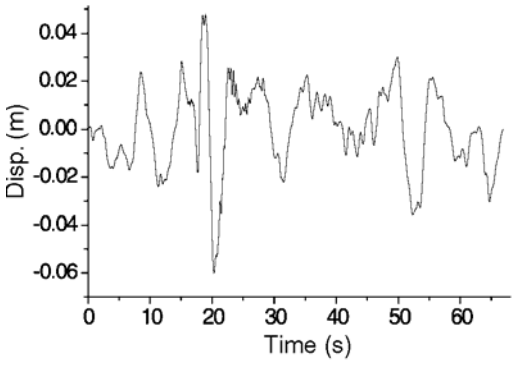

(b) Displacement Disp.1

Fig. 4 Generated ground motions

Having acceleration vector $\ddot{\boldsymbol{x}}_{\mathrm{b}}$ and its corresponding ground displacement, pseudo-static displacement $\boldsymbol{x}_{\mathrm{sa}}$ and dynamic displacement $\boldsymbol{x}_{\mathrm{da}}$ are found from Eqs.(5) and (8), then, the response history of dynamic moment (induced by dynamic displacement), pseudo-static moment (caused by pseudo-static displacement), and the total moment histories are obtained.

3.2.1 Dynamic and total moment

The following response parameters: M_{d}, the maximum absolute value of dynamic moment, and M_{t}, the maximum absolute value of total moment are considered first.

(1) Response for uniform input motion

To study the influence of spatial variability of the ground motions, the structural response due to uniform ground motions is analyzed first to establish a reference response. Therefore, it is assumed that the structure is located on a rigid base and two Cases 1 and 2, with input excitation of Acc.1 and Acc.2, respectively, are analyzed. The results at nodes *A* and *B* (Fig. 1) are presented in Table 1. The average response for Cases 1 and 2 was used as the reference response for uniform ground motion.

Table 1 Response of uniform input motion

	M_{d} (kN·m)		M_t (kN·m)	
Position	*A*	*B*	*A*	*B*
Case 1	78600	73800	78600	73800
Case 2	92300	88100	92300	88100
Case 1*	85450	80950	85450	80950

Case 1* = average of Case 1 and Case 2

Note that for the uniform excitation, the dynamic response and the total response are the same because the pseudo-static response is zero.

(2) Influence of geometric incoherency

To consider the influence of geometric incoherency, it is assumed that the structure is located on a firm (bedrock) site and supports *A* and *D* are excited by Acc.1 and Acc.2 (Case 3), respectively. A fourth case was analyzed with *A* and *D* subjected to Acc.2 and Acc.1, respectively.

In this case, the excitation vector in Eq.(8) is $\ddot{x}_b = [Acc.1 \;\; 0 \;\; 0 \;\; Acc.2 \;\; 0 \;\; 0]^{\mathrm{T}}$, and the inertia force on each node is $m_i(R_{i1}Acc.1 + R_{i2}Acc.2)$. The variation R_{i1} and R_{i2} at different nodes is shown in Fig. 5. The node numbers in the figure refer to the node numbers in the finite element model of the two-column system. Nodes 1-6 and 13-18 are on the left and right columns, respectively. Nodes 7-12 are located at equal spacing on the beam. It is seen that $R_{i1} + R_{i2} = 1.0$. Because the energy of Acc.1 and Acc.2 is concentrated in different time and frequency domains, $R_{i1}Acc.1 + R_{i2}Acc.2$ is not controlled by either Acc.1 or Acc.2. It may be expected that the maximum dynamic response will be smaller than the average of response due to Acc.1 and Acc.2 (Case 1*), which is verified in Fig. 6. As the geometric incoherency induces pseudo-static response, the total response is difficult to predict, but presented in Fig. 7.

Fig.6 shows geometric incoherency makes the dynamic moment much smaller (about 40%-50%) than that of uniform excitation. Fig.7 indicates the total moments at different sections are much larger than those induced by uniform excitation. The

amplification factor ranges from 1.65 to 2.49. For a nonlinear system, these ratios would generally be lower but would still exceed 1.

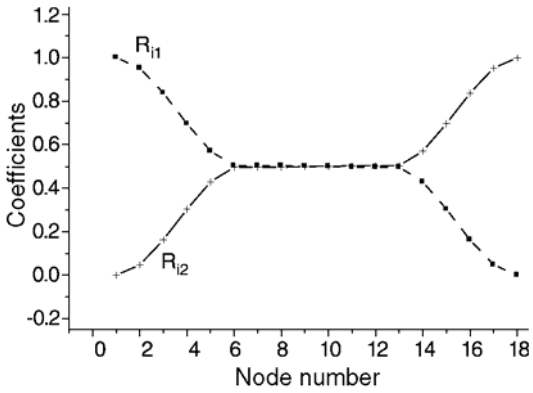

Fig. 5 Coefficients of the effect matrix

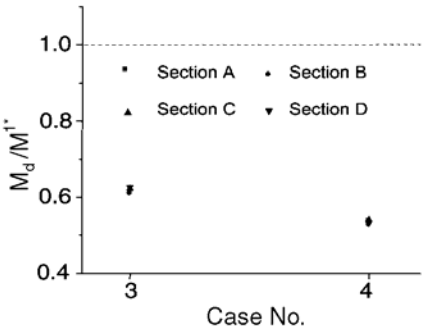

Fig. 6 Dynamic moment ratio

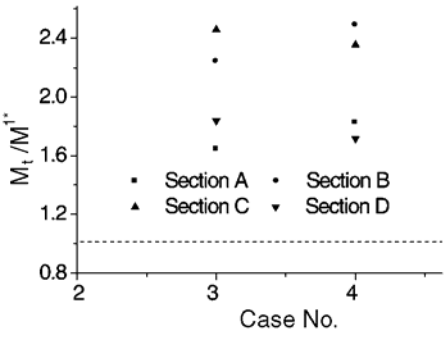

Fig. 7 Total moment ratio

(3) Influence of wave-passage

In this part of the study, it is assumed that earthquake waves arriving at *D* and *A* from source *O* are the same but are delayed relative to each other. The time-delay ΔT of waves arriving *D* and *A* is determined by d / v_{app}, where d is the distance between two supports and v_{app} is the apparent wave velocity.

The wave velocity varies depending on the soil density. Four cases were considered for each input motion of Acc. 1 and Acc. 2. The time-delays from *D* to *A* are 0.28s, 0.14s, 0.06s, 0.00s, corresponding to an apparent velocity of 300m/s, 600m/s, 1200m/s and ∞ (i.e., uniform excitation). Eight cases (5 to 12) were analyzed. The bedrock motion was specified to be Acc.1 in Cases 5-8 and Acc.2 in Cases 9-12. For reasons presented in Section 2, it is expected that the dynamic response with finite apparent velocity will be smaller than that with the infinite apparent velocity (uniform input) and this was verified by the numerical results presented in Yang, *et al*. (2002).

The influence of wave-passage on the total moment is shown in Fig. 8, which indicates that the total moment exceeds that of uniform motion, up to 201%, and reaches its maximum value when the apparent velocity is 300m/s (Cases 5 and 9). It is also shown that the amplification is more pronounced for positions farther from the support (i.e., points *B* and *C*) and the total moment of the first excited column (Sections *D*, *C*) exceeds that of the part excited later.Comparison of the results with those presented in the previous section shows that the influence of wave-passage is smaller than that of geometric incoherency.

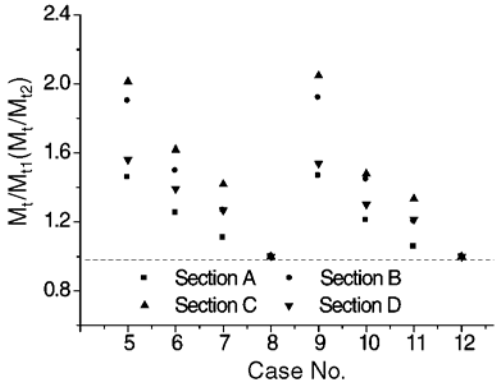

Fig. 8 Influence of wave-passage

(4) Influence of combination of geometric incoherency and wave passage

It is assumed here that the earthquake waves become Acc.1 and Acc.2 with time difference ΔT when they arrive at points *A* and *D* from source *O*. Eight cases (13-20) are analyzed. In Cases 13-16, it is assumed that support *D* is excited by Acc.2 at time *t* and *A* by Acc.1 at time (t-ΔT), while in Cases 17-20 support *D* is excited by Acc.1 at time *t* and *A* by Acc.2 at time (t-ΔT). In these cases, it is difficult to predict the tendency of the response as the combination of both geometric incoherency and wave-passage can be complicated.

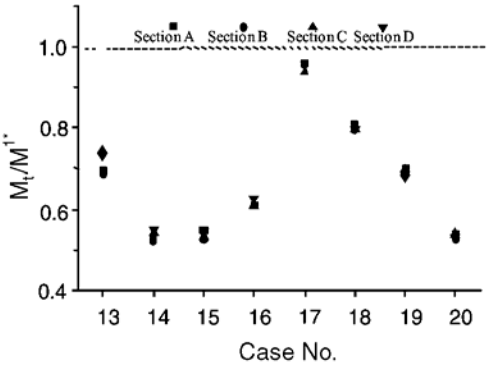

Fig. 9 Influence on dynamic moment

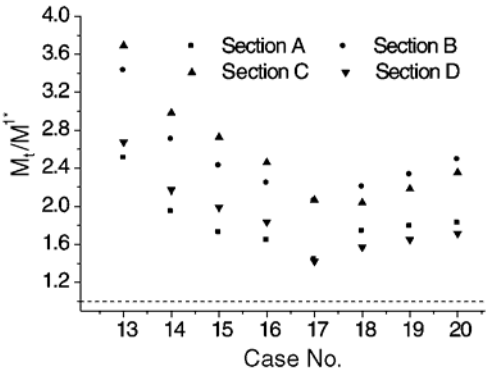

Fig. 10 Influence of total moment

The influence of the combination of geometric incoherency and wave passage is shown in Fig. 9 for dynamic moment and Fig. 10 for total moment. It can be seen that the trend is different for Cases 13-16 and Cases 17-20. In Cases 13-16, dynamic moment decreases and then increases with the increase of apparent velocity. However, the total moment decreases with the increase of apparent velocity. In Cases 17-20, dynamic moment decreases, but the total moment increases with the increase apparent velocity. The dynamic moment in Cases 17-20 is generally larger than Cases 13-16 and total moment in Cases 13-16 is larger with the same apparent velocity.

(5) Influence of local site

To consider the influence of local site, it is assumed that the soil on the top of bedrock of the field is uniform dense sand, but the thickness under two supports is different, 45 m at support *A* and 30 m at support *D*.

The soil column under each support is modeled as a single-degree-of-freedom system with equivalent frequency ω_{sA} =5.343rad/s, ω_{sD} =6.852rad/s, and damping ratio ξ_{sA} =0.128, ξ_{sD} =0.156 for column *A'A* and *D'D* (Joseph, *et al*., 1988; Griffin *et al*., 1995), respectively. With $\ddot{x}_g$ = the acceleration of the bedrock, the input acceleration of the structure is $a_s = \ddot{x} + \ddot{x}_g$, where $\ddot{x}$ is the relative acceleration response of the soil columns under the excitation of $\ddot{x}_g$ and may be determined by:

$$\ddot{x} + 2\xi_s\omega_s\dot{x} + \omega_s^2 x = -\ddot{x}_g \qquad (21)$$

If the bedrock motion is Acc.1, the relative acceleration of points *A* and *D*, a_{A1} and a_{D1}, may be obtained from Eq.(21). Then the absolute acceleration at *A* and *D* are $a_{SA1} = a_{A1} + Acc.1$, $a_{SD1} = a_{D1} + Acc.1$.

To analyze the influence of local site characteristics, the structural response under uniform excitation a_{SA1} (Case 21) and a_{SD1} (Case 22), respectively, are presented in Table 2. When the bedrock motion is Acc.2, then the relative and absolute acceleration of points A and D are a_{A2}, a_{D2}, and a_{SA2}, a_{SD2}. The response of the structure subjected to uniform excitation a_{SA2} (Case 24), a_{SD2} (Case 25) are also presented in Table 2. The average response of Cases 21, 22, and 25, 26, named Case 2^* and 3^*, is also presented in this table, which will be used as the reference response.

The amplitude and the time when the amplitude reaches its maximum value of the input motions, a_{SA1}, a_{SD1}, and a_{SA2}, a_{SD2}, are different, which is not surprising because the motions at the top of the soil columns are different from each other. It is expected that the dynamic response for multi-input motions will be smaller than the averaged uniform response for the reasons presented in Section 2, which has been verified by the numerical results (Yang *et al.*, 2002).

To take the site effect into account, the response of the structure subjected to a_{SA1} (a_{SA2}) at support *A* and a_{SD1} (a_{SD2}) at support *D* (Cases 23, 26) is

Table 2 Results of uniform excitation with different site conditions

Case	21	22	2^*	24	25	3^*	4^*
$D_{max\,B}$(m)	0.1929	0.1704	0.18165	0.2160	0.2357	0.22585	0.20375
$D_{max\,C}$(m)	0.1929	0.1704	0.18165	0.2160	0.2357	0.22585	0.20375
$M_{max\,A}$(kN·m)	367300	324700	346000	410900	448400	429650	387825
$M_{max\,B}$(kN·m)	350000	308400	329200	391600	427100	409350	369275
$M_{max\,C}$(kN·m)	349700	308700	329200	391300	427300	409300	369250
$M_{max\,D}$(kN·m)	367100	324700	345900	411300	448400	429850	387875

calculated and presented in Fig.11. Fig.11 shows that the moments at section *A*, *B* are larger than that of Section *D*, *C*, which is because the ground motion at *A* is larger than that at *D* where the soil column is shorter and soil amplification is smaller. The local site effects make the total moment larger or smaller than that of uniform excitation, depending on the nodal position.

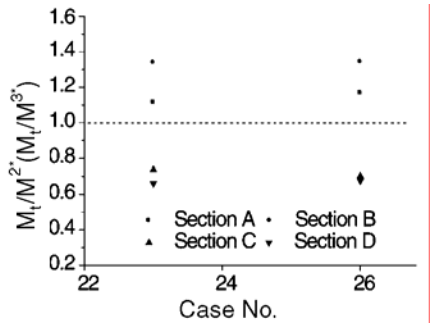

Fig.11 Influence of local-site

(6) Influence of the combination of wave passage and local site

Here, it is assumed that the accelerations of the bedrock corresponding to points *A* and *D* are the same, Acc.1 or Acc.2, but their arrival time is different. Again, four different apparent wave velocities are applied. The input motions are summarized in Table 3. The influence on the moments is illustrated in Fig.12.

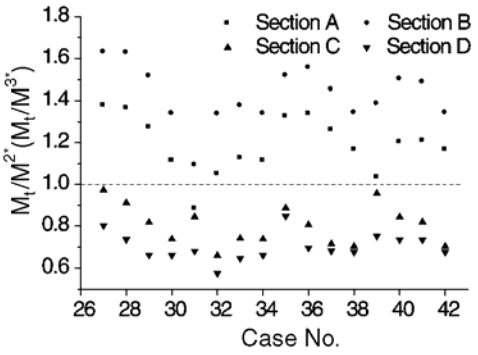

Fig. 12 Influence of combination of wave-passage and local site

Fig.12 shows total moment may be larger or smaller than that of uniform excitation depending on the position in the structure. Wave passage makes the response in the column that is excited first larger, and local site effect makes the response of the part on taller soil column larger. The results also show that the influence of wave passage is not as strong as that of local site. The other results, not presented herein because of space limitation, show dynamic response is still smaller than that of uniform excitation (Yang, *et al*, 2002).

Table 3 Cases to study wave passage and local site effects

Group	I（Acc.1 arrive point *D*' first）			
Case	27	28	29	30 (i.e., Case 23)
Input at support *A*	$a_{SA1}(t-0.28\text{s})$	$a_{SA1}(t-0.14\text{s})$	$a_{SA1}(t-0.06\text{s})$	$a_{SA1}(t)$
Input at Support *D*	$a_{SD1}(t)$			
Group	II （Acc.1 arrive point *A*' first）			
Case	31	32	33	34 (i.e., Case 23)
Input at support *D*	$a_{SD1}(t-0.28\text{s})$	$a_{SD1}(t-0.14\text{s})$	$a_{SD1}(t-0.06\text{s})$	$a_{SD1}(t)$
Input at Support *A*	$a_{SA1}(t)$			
Group	III（Acc.2 arrive point *D*' first）			
Case	35	36	37	38 (i.e., Case 26)
Input at support *A*	$a_{SA2}(t-0.28\text{s})$	$a_{SA2}(t-0.14\text{s})$	$a_{SA2}(t-0.06\text{s})$	$a_{SA2}(t)$
Input at Support *D*	$a_{SD2}(t)$			
Group	IV（Acc.2 arrive point *A*' first）			
Case	39	40	41	42 (i.e., Case 26)
Input at support *D*	$a_{SD2}(t-0.28\text{s})$	$a_{SD2}(t-0.14\text{s})$	$a_{SD2}(t-0.06\text{s})$	$a_{SD2}(t)$
Input at Support *A*	$a_{SA2}(t)$			

(7) Influence of combination of geometric incoherency and local site characteristics

To evaluate the influence of the combination of geometric incoherency and local site characteristics, it is assumed that the excitations of the points on bedrock corresponding to points *A* and *D* are Acc.1 and Acc.2 (Case 43) or Acc.2 and Acc. 1 (Case 44). The inputs to the structure are as shown in Fig. 13.

In this analysis, Case 4* (Table 2), the average of Case 2* and Case 3 *, is used as the reference case with uniform excitation. The results for Cases 43, 44 are shown in Fig.14. The response when two effects are taken into account is larger than that with only local site effect, smaller than that with only geometric incoherency, and smaller or larger than that of uniform excitations depending on the position. Comparing to Cases 3 and 4, in which only geometric incoherency is considered, results show that geometric incoherency and local site features induce opposite effect. Local site modifies the influence of geometric incoherency by increasing the contribution of dynamic response (which is still smaller than that of uniform excitation) and by decreasing the contribution of pseudo-static response.

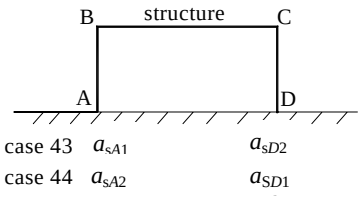

Fig.13 Structure-soil model

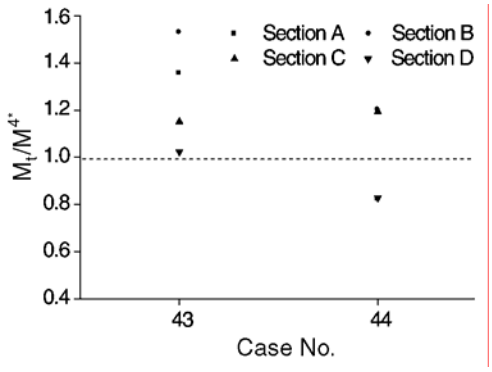

Fig.14 Influence of combination of geometric incoherency and local-site

(8) Influence of the combination of geometric incoherency, wave passage, and local site

Four groups, each with four combinations leading to 16 cases (45-60) similar to those in Table 3 but with geometric incoherency, are considered. Fig.15 shows these four groups. Results are presented in Fig. 16.

Comparing Cases 45-47, 49-51 to Case 43 (i.e., Cases 48 and 52); 53-55, 57-59 to Case 44 (i.e., Cases 56 and 60), it is found that the varying tendency of response depending on apparent velocity still exists, while the ratios are smaller than Fig.12. Comparing to Fig.12, geometric incoherency increases the total moment; comparing to Fig.10, local site effects decrease the total moment. Fig.16 also indicates that in about 80% of the sections incoherent moment increase up to 80% and in 20% of sections incoherent moment reduces up to 50%.

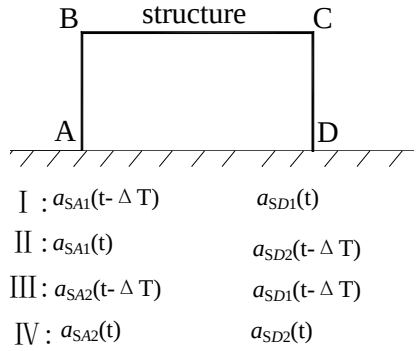

Fig.15 Structure-soil model

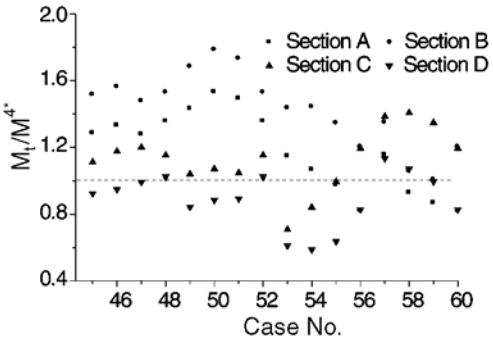

Fig.16 Influence of incoherency

3.2.2 Relationship between dynamic, pseudo-static, and total moment

To identify response trends that can potentially be applied in practical design, the ratio of the maximum values of dynamic moment to total moment, M_d / M_t, and the ratio of the maximum value of pseudo-static moment to total moment, M_p / M_t, are calculated. Note that the maxima are found regardless of time of occurrence. Meanwhile, the ratios of dynamic and pseudo-static moment at the time when the total moment reaches its maximum absolute value, denoted as t_{max}, to the maximum total moment $\frac{M_d(t_{max})}{M_t(t_{max})}$, $\frac{M_p(t_{max})}{M_t(t_{max})}$ are also investigated to check their contributions to the maximum response.

If there is some trend for these ratios, the response under the incoherent ground motions can be

represented by dynamic or pseudo-static response, which is relatively easy to obtain. The results for the above 60 cases are illustrated in Figs. 17 and 18.

Figs.17 and 18 show that when local site effect is not included, some trends may be found (Cases 3-20), while when all three factors are considered, the ratios distribute randomly and no consistent trends exist. These figures also show these ratios may be larger than 1.0 or smaller than 0.0, which means the dynamic and pseudo-static response may be out of phase.

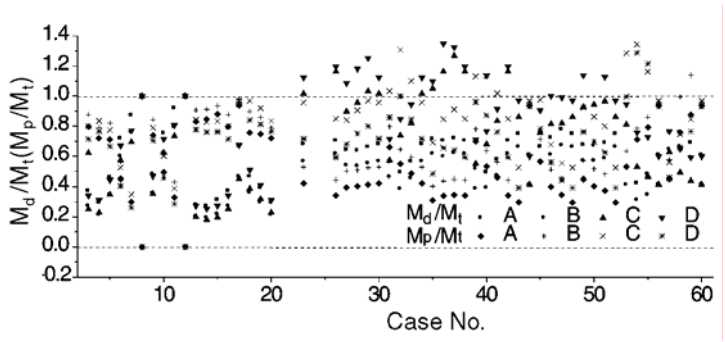

Fig.17 Relationship of the maximum values of dynamic, pseudo-static, and total moment

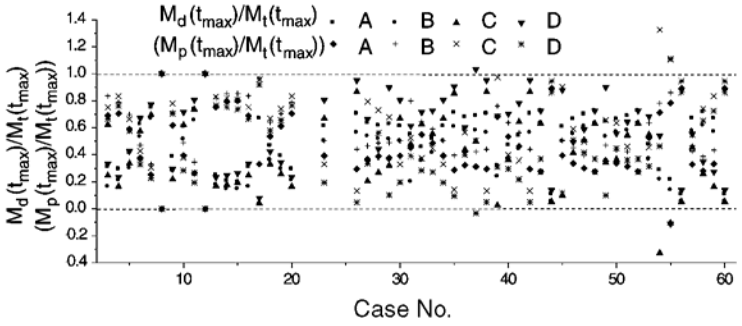

Fig.18 Relationship of dynamic, pseudo-static, and total moment at $t_{\max}$

4 Effect of incoherent ground motion in a 24-span bridge

The study of the two-support system described in the previous section was aimed at determining any general trends. The issue of incoherent ground motion effect is usually of interest in multi-support systems with a relatively long distance between the extreme supports. The analytical procedure described in Section 2 was applied to a linear model of a multi-span bridge. The downtown viaduct in Las Vegas, Nevada, USA, is a 24-span, 500m long bridge (Fig.19), which was built in 1969. The bridge has severe shortcomings with respect to seismic detailing. Among the issues studied in evaluating the bridge was the effect of spatial variability of ground motions (Saiidi *et al*., 2002).

To simplify the analysis, each frame between adjacent hinges is modeled as a single lumped mass and the associated columns are replaced by one column. Hence, the viaduct is reduced to a seven-span bridge. Logs of test borings at the bridge site showed the topsoil is “soft” on the left part and “medium firm” on the right part corresponding to Type III and Type II of UBC 2000, respectively. Similar to what was done for the one-span frame, the topsoil column under each support is modeled as a single-degree-of-freedom system. The structure-soil model is presented in Fig.20.

In Fig. 20, M_i (i=1,2,…8) represent the deck mass and H_i (i= 1,2,3and 4) are the heights. P_i (i= 1,2,3and 4) refers to the pier number. After the structural parameters are specified, the influence matrix Eq.(5) is determined (Fig.21), which indicates that the coefficients are influenced by structural stiffness and the relative position of the node to the supports. It is shown that ground acceleration at support 8 has the maximum effect among all supports.

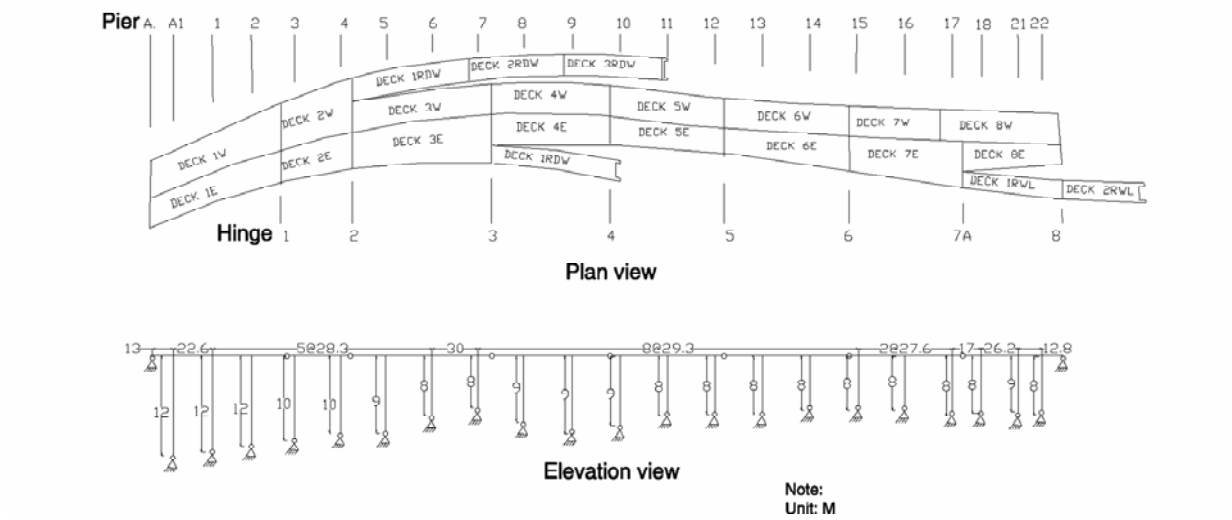

Fig. 19 Structural plan and elevation

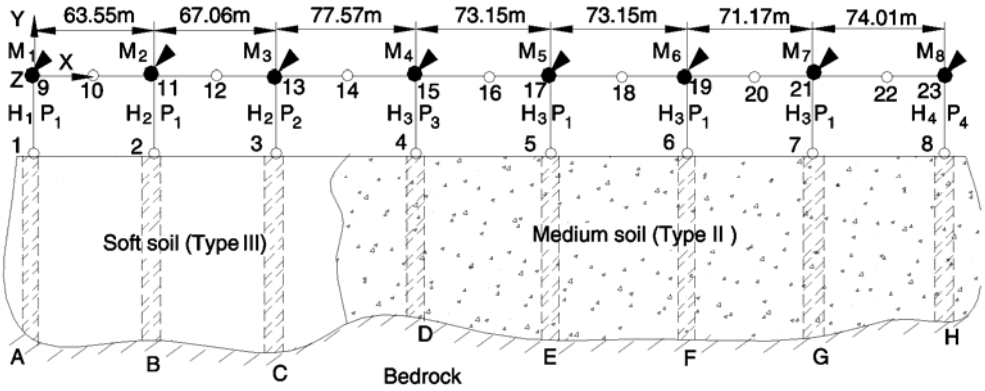

Fig. 20 Multi-support structure-soil model

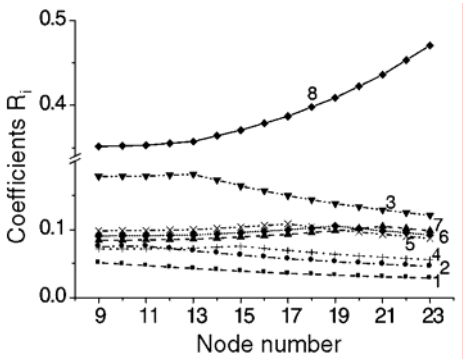

Fig. 21 Influence coefficients

generated based on the same parameters as those used for the two column frame. The comparison of the target coherency function and that of the generated acceleration history is presented in Fig.22.

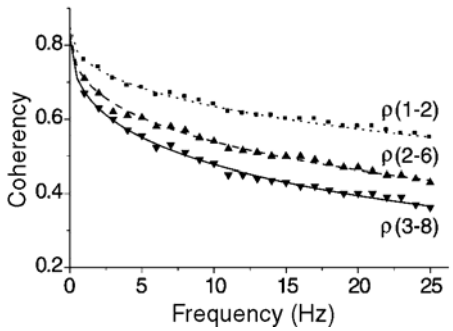

Fig. 22 Coherency function

4.1 Incoherent ground motions

Eight acceleration histories of the bedrock at Points *A* to *H* (Fig.20), denoted as Acc.1, Acc.2, , Acc.8, corresponding to the bridge supports (Points 1 to 8), satisfying coherency function Eq.(12), are

After the bedrock accelerations are generated, the motion of the topsoil is obtained from the filtered equation. Here, the soil column under each support is modeled as a SDOF system with equivalent

frequencies and damping ratios for soft and medium soil columns specified as ω_{gs} = 5.0 rad/s, ω_{gm} = 10.0 rad/s, and ξ_{gs} = 0.2, ξ_{gm} = 0.4 (Monti *et al*., 1996), respectively.

4.2 Parametric studies

The same response parameters as those of the one-span frame, namely, dynamic, pseudo-static, and total response, are studied. Similar conclusions may be reached for the relation of dynamic, pseudo-static, and total force. Therefore, only the base shear at each support is presented and discussed.

(1) Influence of local site characteristics

To analyze the influence of the local site, the earthquake acceleration at point E (Fig.20), i.e., Acc. 5, is selected as representative of the uniform input to the topsoil at all supports. The acceleration relative to the bedrock, denoted as a_s for support 1 to 3 and a_m for support 4 to 8, is obtained from Eq.(21). The acceleration inputs to the structure at the footings are $a_{s5} = a_s + Acc.5$ at supports 1 to 3, and $a_{m5} = a_m + Acc.5$ at supports 4 to 8. Then the displacements, D_{s5} and D_{m5}, corresponding to acceleration a_{s5} and a_{m5} are obtained. The structural response for three input cases (Case 1: uniform input, a_{s5}; Case 2: uniform input, a_{m5}; Case 3: non-uniform input, a_{s5} for supports 1-3, a_{m5} for supports 4-8) is analyzed. The maximum base shears for the uniform input are listed in Table 4.

Table 4 Maximum base shears (F_t, i.e., F_d) for uniform excitations (kN)

Section position	Case 1	Case 2	Case 5*
1	3031	1742	2386
2	4788	2749	3768
3	12230	7006	9618
4	5320	3037	4178
5	7764	4412	6088
6	7529	4258	5893
7	7259	4088	5673
8	30550	17170	23860

* average of Case 1 and Case 2

In Case 3, only the local-site effect is considered, the ratios of the shear forces for the non-uniform to uniform excitation are presented in Fig. 23. It can be seen that the base shear is reduced due to the local soil characteristics by at least 15% at all supports.

(2) Influence of combination of wave passage and local site characteristics

Even though the topsoil is specified to be Type II and III, the values of standard penetration tests in the right and left parts do not differ greatly, and they are close to the border value of Type II and III. It is assumed here $v_{app} = 600$ m/s for the entire bridge. Two cases are analyzed. It is assumed that the wave propagates from support 8 to 1 in Case 4 and from support 1 to 8 in Case 5. The results are presented in Fig. 23. It is shown that wave passage makes the base shears larger in a few supports and smaller in most of the supports except for those where local site effect is considered alone. It may be inferred that the response is smaller than that of uniform excitation.

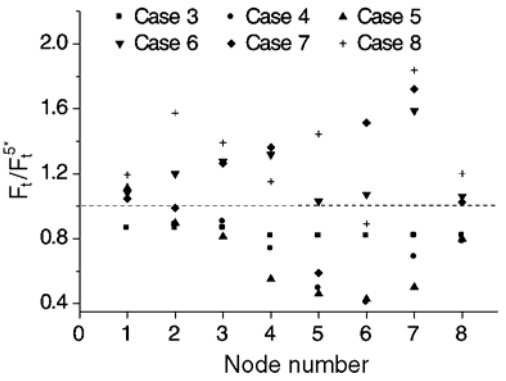

Fig. 23 Incoherent influence on seven-span system

(3) Influence of Combination of Geometric Incoherency and Local Site Characteristics

After the eight generated time histories corresponding to the eight supports are filtered by soft or medium soil columns, the column base input accelerations $a_{s1}, a_{s2}, a_{s3}, a_{m4}, a_{m5}, a_{m6}, a_{m7}, a_{m8}$ and their corresponding displacements are obtained; then, the structure is analyzed (Case 6). Shown in Fig. 23 are the base shear ratios normalized to the shear forces for uniform motion. When geometric incoherency is added to site effect, the base shears are amplified and are equal to or larger than those of uniform excitation by up to 60%.

(4) Influence of combination of wave passage, geometric incoherency, and local site characteristics

Based on Section 3, wave passage effect is added, and two Cases (Case 7: wave propagates from support 8 to 1; Case 8: wave propagates from support 1 to 8) are analyzed. The results are presented in Fig. 23. Regardless of the direction of the wave, the base shears of most supports in these two cases exceed those of uniform excitation by up to 80%. However, there are a few sections whose response are still smaller than that of uniform excitation.

From the numerical results, it is concluded for the seven-span system that when the geometric incoherency is not considered (Cases 3, 4, 5), base shear in most supports is smaller than that of uniform excitation; when geometric incoherency and local site effect are included (Case 6, 7, 8), base shear in some supports is larger than that of uniform excitation; when

all three factors are considered, shear force reaches its maximum value in most sections and is larger than that of uniform inputs by up to 80%. However, there are still some supports in which the base shear force is smaller than that of uniform excitation by up to 50%.

5 Conclusions

Influence of incoherency of ground motion on a one-span frame and a seven-span system is studied systematically. Approximately 70 cases are analyzed. The following conclusion may be reached based on the results:

The incoherency of earthquake ground motion can have a dramatic influence on structural response by modifying the dynamic response to uniform excitation and inducing pseudo-static responses which do not exist in structures subjected to uniform excitation.

The effects of the three factors which result in the earthquake ground motion incoherency are different. When considered individually, all of them induce pseudo-static response and a smaller dynamic response than that of uniform excitation. While the magnitude is different, geometric incoherency and local site characteristics have stronger influence than wave passage effect.

When wave passage effect is considered with geometric incoherency, or local site effect, wave passage effect will amplify or de-amplify the influence of the other factor according to the relation of wave traveling direction to the structural axis. No apparent trend in the variation of the response as a function of the apparent velocity can be found.

When geometric incoherency and local site effects are considered simultaneously, local site effect increases the dynamic response and decreases pseudo-static response compared to when geometric incoherency alone is considered.

When all the three effects are taken into account, the results are similar to those of cases with only geometric incoherency and local site effect. The wave passage does not appear to influence the response significantly.

Dynamic response and pseudo-static response may be in phase or out of phase, which makes their contribution to the total response highly variable.

The total response when ground motion incoherency is considered may be larger or smaller than that of uniform excitation, the magnitude of which depends on the position, the response, soil conditions and ground motion. For the cases studied here, the total internal forces are 60% to 180% of that of uniform excitation, and the pseudo-static response dominates the response by contributing approximately 60% to 80% of the total response. It is also shown that for the cases studied in this article, the responses of 80% of nodes and sections are larger than those of uniform excitation.

6 Acknowledgements

The first authors would like to express appreciation for the financial support from the China Scholarship Council and the Teaching and Research Award Program for Outstanding Young Teachers (TRAPOYT) in Higher Education Institutions of MOE, PRC. The authors would also like to thank the support of the Nevada Department of Transportation. The assistance by Mr. Gregory L. Griffin, OBEC Consulting Engineers of Portland, Oregon, and Prof. John Anderson, Director of Seismology Laboratory, University of Nevada, Reno, is also appreciated

References

Abdel-Ghaffar A and Nazmy AS (1991), "3-D Nonlinear Seismic Behavior of Cable-Stayed Bridge," *Journal of Structural Engineering*, ASCE, **117**(11): 3456-3476.

Abrahamson NA, Bolt BA, Darragh RB, Penzien J and Tsai Y B (1987), "The SMART-1 Accelerograph Array (1980-1987): A Review," *Earthquake Spectra*, **3:** 267-287.

Banerji P, Murudi MA, Shah and Popplewell N (2000), "Tuned Liquid Dampers for Controlling Earthquake Response of Structures," *Earthquake Engineering and Structural Dynamics*, **29:** 587-60

Behnamfar F and Sugimura Y (1999), "Dynamic Response of Adjacent Structures Under Spatially Variable Seismic," *Probabilistic Engineering Mechanics*, **14**: 33-44.

Beresnev IA, Wen L and Yeh YT (1994), "Source, Path and Site Effects on Dominant Frequency and Spatial Variation of Strong Ground Motion Recorded By SMART1 And SMART2 Arrays in Taiwan, " *Earthquake Engineering and Structural Dynamics*, **23:** 583-597.

Bogdanoff JL, Goldberg JE and Schiff (1965), "The Effect of Ground Transmission Time on The Response of Long Structures," *Bull Seism Soc Am*, **55**(3): 627-640.

Clough R and Penzien J (1975), *Dynamics of structures*, McGraw-Hill, New York, N. Y..

Der Kiureghian A (1996), "A Coherency Model for Spatially Varying Ground Motions," *Earthquake Engineering and Structural Dynamics*, **25:** 99-111.

Ettouney M, Hapij A and Gajer R (2001), "Frequency Domain Analysis of Long-Span Bridges Subjected to Non Uniform Seismic Motions, " *J. of Bridge Engineering*, **6**(6): 577-586.

Griffin G, Saiidi M and Maragakis E(1995), "Nonlinear Seismic Response Analysis of Isolated Bridges with Multiple Columns, " *Report No. CCEER-95-6*, Engineering Research and Development

Center, University of Nevada, Reno.

Hao H (1989), "Effects of Spatial Variation of Ground Motions on Large Multiply-Supported Structures," *Report, UCB/EERC-89/06*, University Of California, Berkeley.

Hao H (1998), "Response of Two-Way Eccentric Building to Nonuniform Base Excitations, " *Engineering Structures*, **20**(8): 677-684.

Hao H and Zhang S (1999), "Spatial Ground Motion Effect on Relative Displacement of Adjacent Building Structures," *Earthquake Engineering and Structural Dynamics*, **28:** 333-349.

Harichandran RS, Hawwari A and Sweiden BN (1996), "Response of Long-Span Bridges to Spatially Varying Ground Motion," *J. of Structural Engineering*, **122**(5): 476-484.

Joseph I, Sun, R Golesorkhi H and Bolton Seed (1988), "Dynamic Moduli and Damping Ratios for Cohesive Soils," *Report No. UCB/EERC-88/15*, University of California, Berkeley.

Kahan M, Gibert R and Bard P (1996), "Influence of Seismic Waves Spatial Variability on Bridges: A Sensitivity Analysis,"*Earthquake Engineering and Structural Dynamic*, **25**(4): 795-814.

Luco JE and Wong LH (1986), "Response of A Rigid Foundation to A Spatially Random Ground Motion, " *Earthquake Engineering and Structural Dynamics*, **14:** 891-908.

Monti G, Nuti C and Pinto P (1996), "Nonlinear Response of Bridges Under Multi-Support Excitation," *J. Structural Engineering*, **122**(10): 1147-1159.

Nazmy A and Abdel-Ghaffar A (1992), "Effect of Ground Motion Spatial Variability on The Response of Cable-Stayed Bridges," *Earthquake Engineering and Structural Dynamics*, **21**:1-20.

Ohsaki Y (1979), "On the siginificance of Phase Content in Earthquake Ground Motion, " *Earthquake Engineering and Structural Dynamics*, **7**(5): 427-439.

Perotti F (1990), "Structural Response to Non-Stationary Multiple-Support Random Excitation," *Earthquake Engineering and Structural Dynamics*, **19**(4): 513-527.

Price T and Eberhard M (1998), "Effects of Spatially Varying Ground Motions on Short Bridges," *J. Structural Engineering*, **124**(8): 948-955.

Saiidi M, Itani A, Yang Q, and Ladkany S, "Multifaceted Seismic Evaluation and Retrofit Study of A Major Viaduct," *Proceedings, First International Conference and Annual Meeting of Asian-Pacific Network of Centers for Earthquake Engineering Research*, Harbin, China, August 2002.

Shrikhande M and Gupta V (1999), "Dynamic Soil-Structure Interaction Effects On The Seismic Response of Suspension Bridges," *Earthquake Engineering and Structural Dynamics*, **28:** 1383-1403.

Wilson E (2000), *Three Dimensional Static and Dynamic Analysis of Structures*, A publication of computer and structures. Inc., April.

Yang Q and Chen Y (2000), "A Practical Coherency Model for Spatially Varying Ground Motions," *Structural Engineering and Mechanics*, **9**(2):141-152.

Yang Q and Jiang H (2001), "Generation of Ground Motion Non-Stationary Both in Time and Frequency Domains Based on Phase Difference Spectrum," *Earthquake Engineering and Engineering Vibration*, **21(**3): 10-16, Harbin. (in Chinese)

Yang Q, Saiidi M, Wang H and Itani A(2002), "Influences of Earthquake Ground Motion Incoherency on Multi-support Structures," *Report Number CCEER-02-2*, Center for Civil Engineering Earthquake Research, Department of Civil Engineering, University of Nevada.

Zerva A (1990), "Response of Multi-Span Beams to Spatially Incoherent Seismic Ground Motions," *Earthquake Engineering and Structural Dynamics*, **19:** 819-832.

Zhao Fengxin (1992), "The Phase Difference Spectrum of Time Histories and the Generation of the Design Ground Motions", *Ph.D. Dissertation*, Institute of Geophysics, China Seismology Bureau(in Chinese).